

# Supporting Information

## Remarkable solid-state fluorescent change from visible to near-infrared region based on the protonation/deprotonation of AlEgen

Yangyang Li,<sup>‡a</sup> Xian Wang,<sup>‡a</sup> Lei Zhang,<sup>b,c</sup> Luqi Liu,<sup>a</sup> Qiusheng Wang,<sup>a</sup> Hongguang Lu<sup>\*a</sup> and Xiaowei Zhao<sup>\*a</sup>

# Supporting Information

## Contents

1. Experimental section .....	S1
2. View of the molecular stacking structure in single crystal of DPP3A .....	S3
3. Absorption and fluorescence spectra of DPP3A in THF solution .....	S3
4. DLS and SEM studies of DPP3A in the THF/water mixture .....	S4
5. Absorption and fluorescence spectra of DPP3A in different solution .....	S4
6. Time-resolved fluorescence of DPP3A in DMF and in crystal .....	S5
7. Summary of quantum yield and fluorescent lifetime of DPP3A in DMF and in crystal .....	S5
8. <sup>1</sup> H NMR and HRMS of DPP3A-H .....	S6
9. Maximum emission wavelength changes of DPP3A versus repeating HCl/NH <sub>3</sub> cycles .....	S7
10. Characterization of compound DPP3A .....	S8
11. References .....	S9

## Experimental Section

### 1.1 General information

All chemicals and solvents were commercially available and were used without further purification. 3-Pyridineacetonitrile was purchased from Heowns. 2,5-Bis(diphenylamino)terephthalaldehyde was synthesized according to the literature.<sup>[1]</sup>

Melting point was measured by differential scanning calorimetry (DSC, NETZSCH F3200). <sup>1</sup>H NMR spectra were recorded with a Bruker AV-400 (400 MHz) spectrometer at room temperature with tetramethylsilane (TMS,  $\delta = 0$  ppm) as an internal standard. <sup>13</sup>C NMR spectra were determined on a Bruker AV-400 (100 MHz) spectrometer with tetramethylsilane (TMS,  $\delta = 0$  ppm) as an internal standard. High resolution mass spectra (HRMS) were performed on a Waters Xevo Q-TOF MS with an ESI source. UV-vis spectra were recorded on a Shimadzu UV-3390 spectrophotometer. Fluorescence spectra and time-resolved fluorescence spectra were carried out with an Edinburgh FLS1000 spectrometer. Crystalline state fluorescence efficiency was measured using an Edinburgh FLS1000 spectrometer with an integrating sphere. Dynamic light scattering (DLS) measurement was performed using a Malvern Nano-ZS instrument at room temperature. The morphology of NPs was observed using a Zeiss MERLIN Compact type field emission scanning electron microscope (SEM). Density functional theory (DFT) calculations were carried out using the Gaussian 09 package (Revision D.01). The geometries were optimized at the B3LYP/6-31G\*\* level.<sup>[2]</sup>

Single crystal of fluorophore DPP3A suitable for X-ray structural analysis was obtained by the slow diffusion of hexane vapor into CH<sub>2</sub>Cl<sub>2</sub> solution. Single crystal X-ray diffraction intensity data was collected on a Rigaku XtaLAB PRO diffractometer with Cu K $\alpha$  radiation. CCDC 1979104 (DPP3A) contains the supplementary crystallographic data for this paper. The data can be obtained free of charge from the Cambridge Crystallographic Data Centre via [www.ccdc.cam.ac.uk/data\\_request/cif](http://www.ccdc.cam.ac.uk/data_request/cif).

### 1.2 Synthesis of (2Z,2'Z)-3,3'-(2,5-bis(diphenylamino)-1,4-phenylene)bis(2-(pyridin-3-yl)acrylonitrile) (DPP3A)

A flask was charged with a solution of 3-pyridineacetonitrile (4.260 mmol, 0.503 g) and 2,5-bis(diphenylamino)terephthalaldehyde (2.130 mmol, 1.000 g) in ethanol (40 mL).

Sodium hydroxide (33.080 mmol, 1.320 g) dissolved in ethanol (20 mL) was added dropwise to the stirred solution. The mixture was stirred for 1 h at room temperature under N<sub>2</sub> and then was concentrated under reduced pressure. The concentrate was cooled in a refrigerator to obtain a red solid. The precipitate was filtered and washed with water and ethanol. The crude product was purified by recrystallization from CH<sub>2</sub>Cl<sub>2</sub> to yield the desired product. Yield: 82%, a red solid. Mp > 300 °C. <sup>1</sup>H NMR (400 Hz, CDCl<sub>3</sub>, TMS, ppm): δ 8.51-8.52 (d, *J* = 4.0 Hz, 2H), 8.35 (s, 2H), 7.74 (s, 2H), 7.48-7.51 (m, 4H), 7.27-7.31 (t, *J* = 8.0 Hz, 8H), 7.22-7.24 (m, 2H), 7.10-7.12 (d, *J* = 7.6 Hz, 8H), 6.99-7.03 (t, *J* = 7.2 Hz, 4H); <sup>13</sup>C NMR (100 MHz, CDCl<sub>3</sub>, TMS, ppm): δ 150.00, 147.52, 146.82, 143.40, 140.92, 140.76, 133.35, 132.91, 129.71, 128.75, 123.31, 123.25, 119.22, 115.96, 111.50; HRMS (ESI): *m/z*: Calcd for C<sub>46</sub>H<sub>33</sub>N<sub>6</sub>: 669.2767 [*M*+H]<sup>+</sup>; Found: 669.2772.

## 2. View of the molecular stacking structure in single crystal of DPP3A

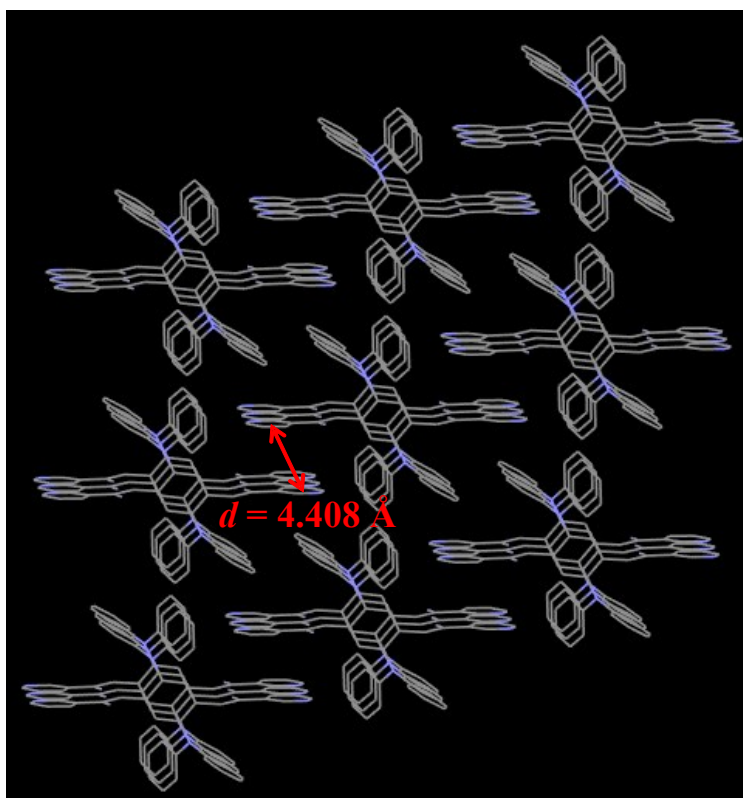


**Figure S1.** View of the molecular stacking structure in single crystal of DPP3A. Hydrogens are omitted for clarity.

## 3. Absorption and fluorescence spectra of DPP3A in THF solution

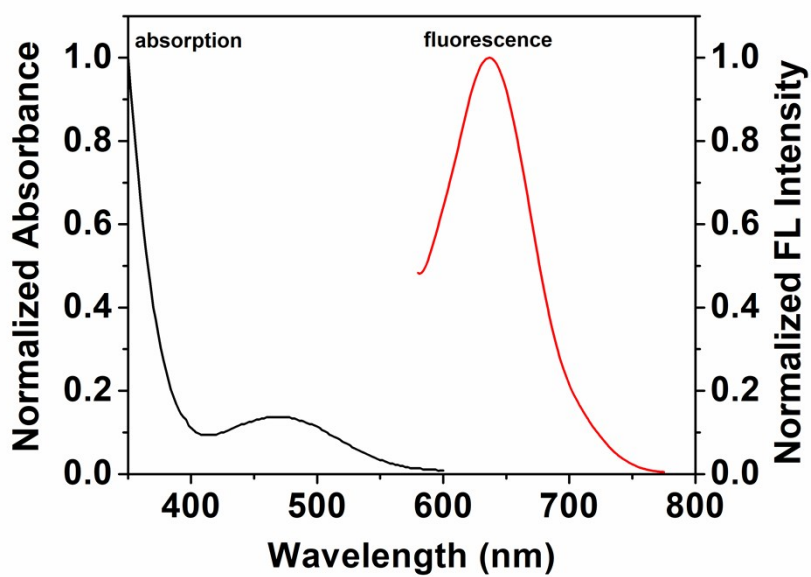


**Figure S2.** Absorption and fluorescence spectra of DPP3A in THF solution.

#### 4. DLS and SEM studies of DPP3A in THF/water mixture

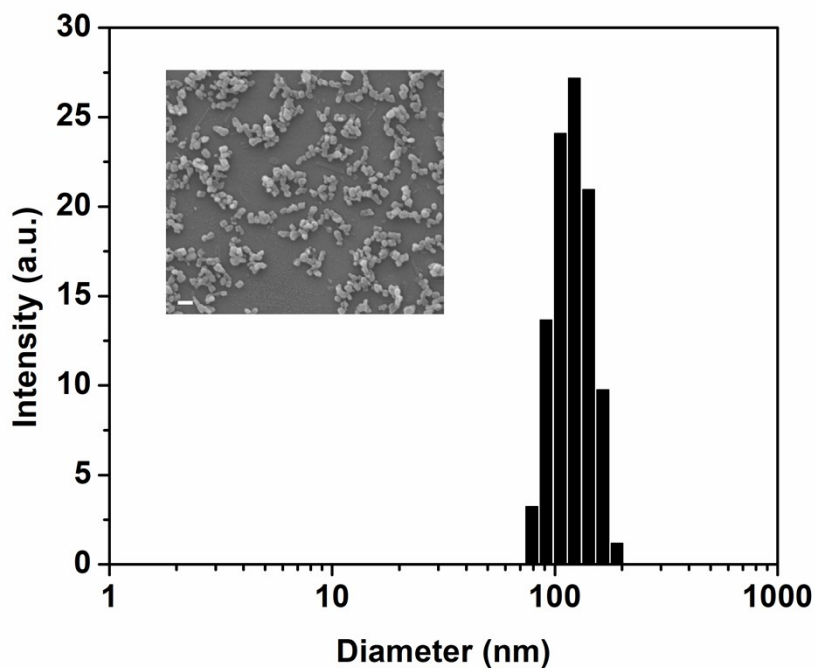


**Figure S3.** Particle size distribution and morphological structure of DPP3A in THF/water ( $v/v = 5/95$ ) mixture studied by DLS and SEM (inset, scale bar is 200 nm).

#### 5. Absorption and fluorescence spectra of DPP3A in different solution

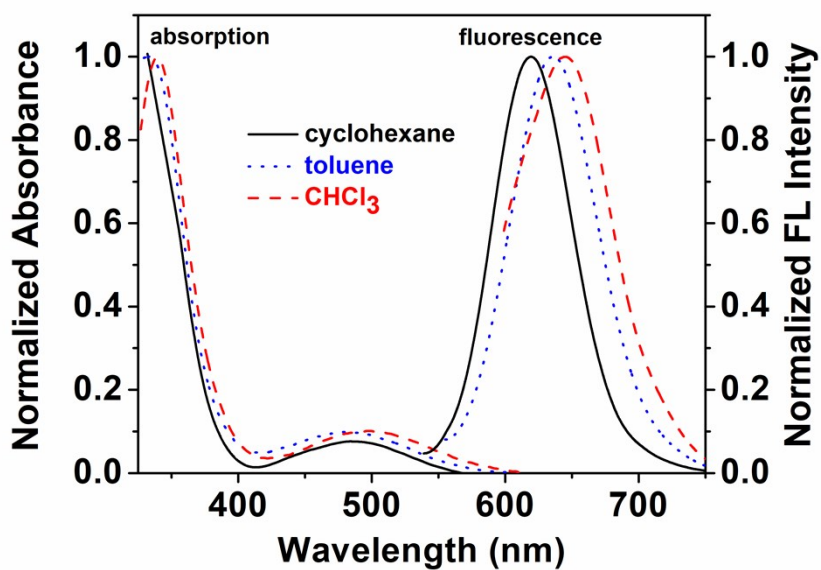


**Figure S4.** Absorption and fluorescence spectra of DPP3A in different solution.

## 6. Time-resolved fluorescence of DPP3A in DMF and in crystal

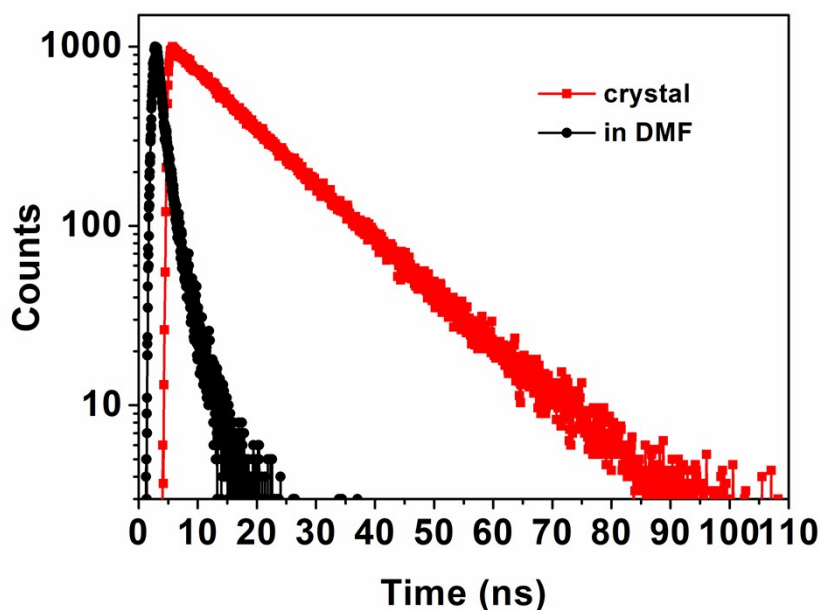


Figure S5. Time-resolved fluorescence of DPP3A in DMF and in crystal.

## 7. Summary of quantum yield and fluorescent lifetime of DPP3A in DMF and in crystal

Table S1. Summary of quantum yield and fluorescent lifetime of DPP3A in DMF and in crystal

Sample	$\Phi_F$ (%)	$\langle\tau\rangle$ (ns)	$K_r$ ( $s^{-1}$ )	$K_{nr}$ ( $s^{-1}$ )
<b>DMF solution</b>	0.29	2.00	$1.450 \times 10^6$	$4.986 \times 10^8$
<b>Crystal</b>	48.6	14.08	$3.452 \times 10^7$	$3.651 \times 10^7$

Abbreviations: fluorescence quantum yield:  $\Phi_F$ . Average lifetime:  $\langle\tau\rangle = (A_1\tau_1^2 + A_2\tau_2^2)/(A_1\tau_1 + A_2\tau_2)$ . Radiative transition rate constant:  $K_r = \Phi_F/\langle\tau\rangle$ . Non-radiative transition rate constant:  $K_{nr} = (1 - \Phi_F)/\langle\tau\rangle$ .

## 8. <sup>1</sup>H NMR and HRMS of DPP3A-H

DPP3A easily transforms into the protonated DPP3A-H after fuming with HCl vapor, which was confirmed by <sup>1</sup>H NMR spectrum and HRMS. <sup>1</sup>H NMR (400 Hz, DMSO, TMS, ppm):  $\delta$  8.83-8.84 (d,  $J = 4.0$  Hz, 2H), 8.80 (s, 2H), 8.35-8.37 (d,  $J = 7.6$  Hz, 2H), 8.18 (s, 2H), 7.94-7.98 (m, 2H), 7.64 (s, 2H), 7.22-7.26 (t,  $J = 7.6$  Hz, 8H), 7.06-7.09 (d,  $J = 8.0$  Hz, 8H), 6.92-6.95 (t,  $J = 7.2$  Hz, 4H); HRMS (ESI):  $m/z$ : Calcd for C<sub>46</sub>H<sub>34</sub>N<sub>6</sub>: 670.2845 [ $M-2Cl$ ]<sup>2+</sup>; Found: 335.1432.

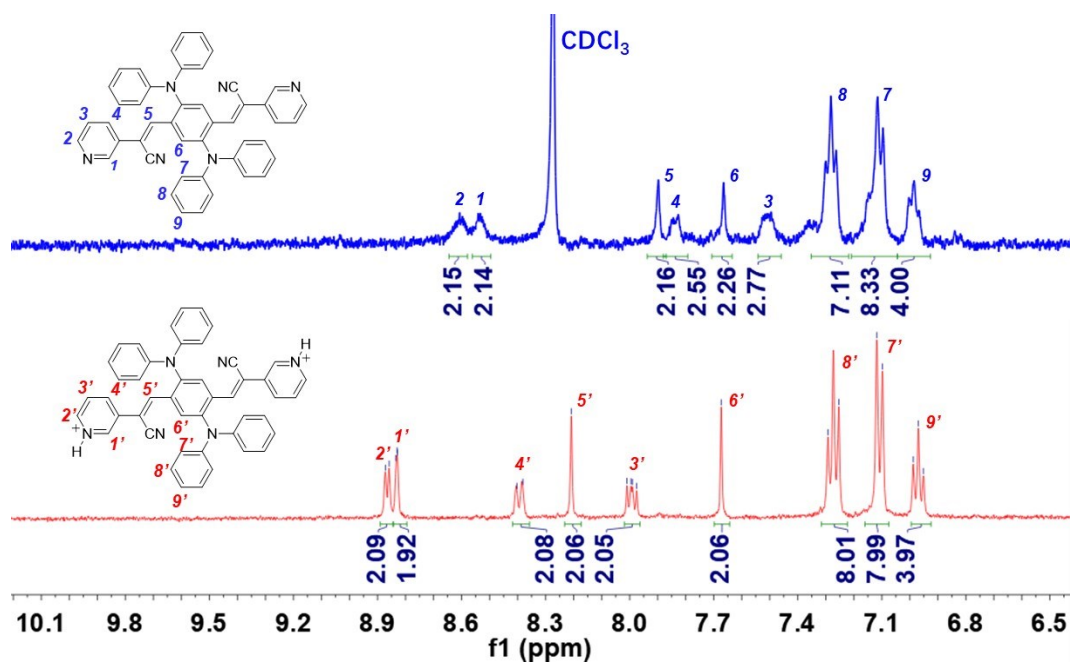


**Figure S6.** <sup>1</sup>H NMR spectra of DPP3A in DMSO-*d*<sub>6</sub> and CDCl<sub>3</sub> solution ( $v:v = 4:1$ , CDCl<sub>3</sub> solvent was used to improve the solubility of DPP3A) and protonated DPP3A-H in DMSO-*d*<sub>6</sub> solution.

### 9. Maximum emission wavelength changes of DPP3A versus repeating HCl/NH<sub>3</sub> cycles

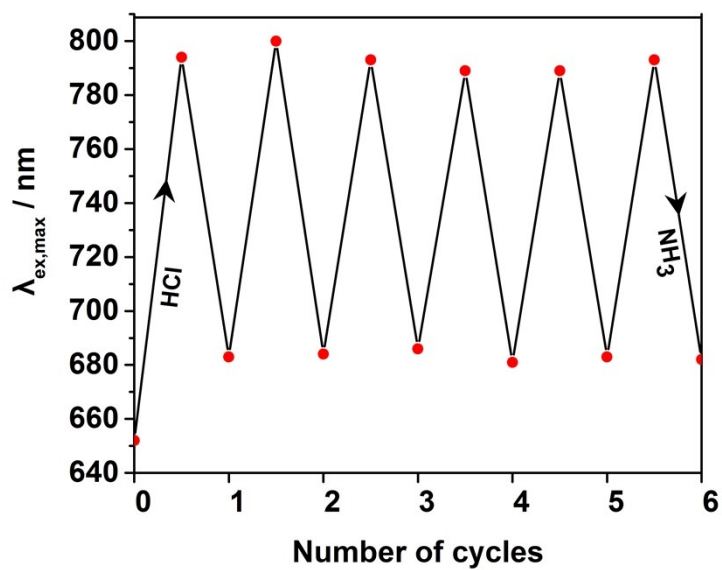


**Figure S7.** Maximum emission wavelength changes of DPP3A versus repeating HCl/NH<sub>3</sub> cycles.

## 10. Characterization of compound DPP3A

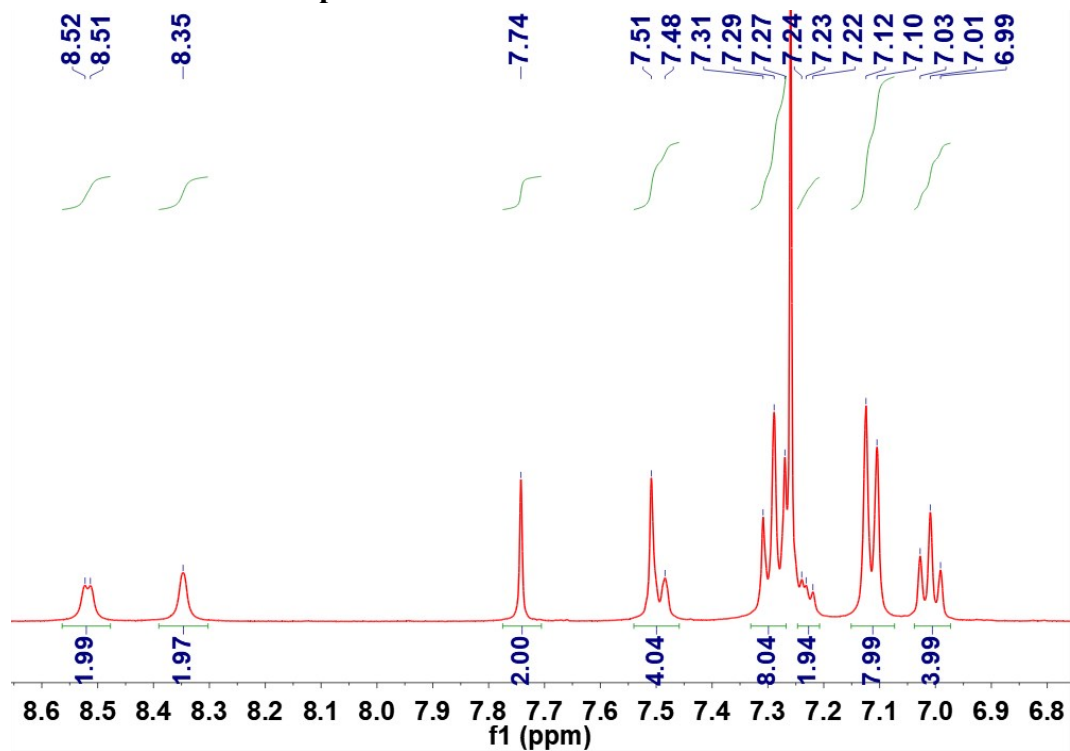


Figure S8. <sup>1</sup>H NMR spectrum of compound DPP3A in CDCl<sub>3</sub>.

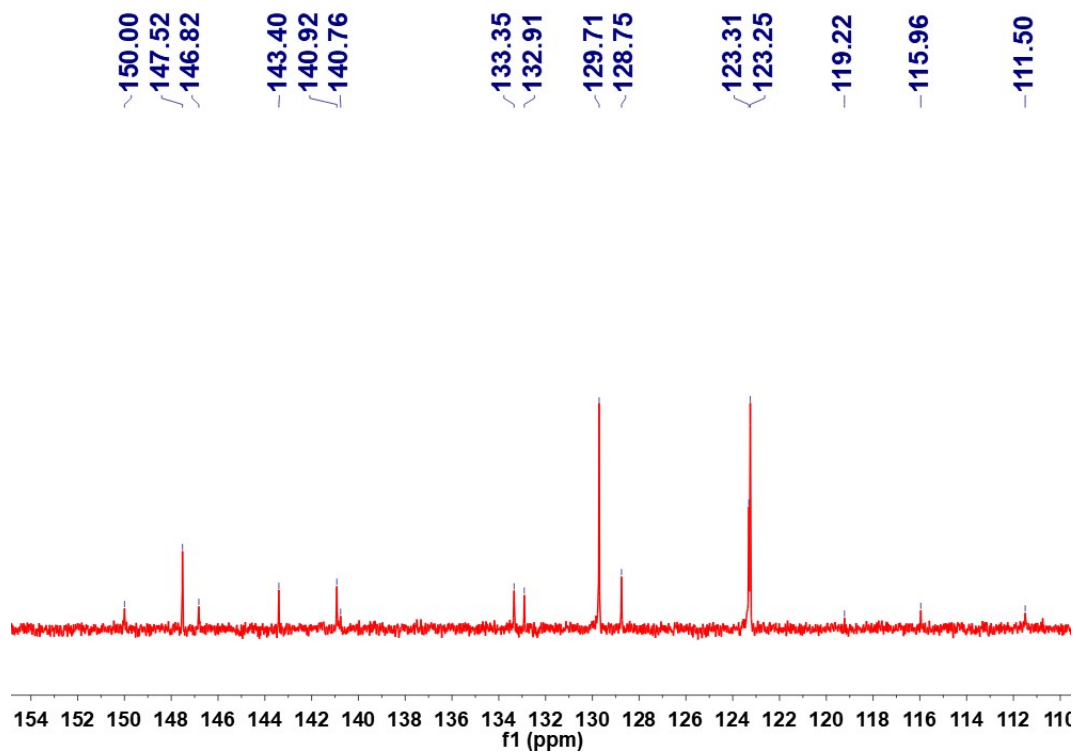


Figure S9. <sup>13</sup>C NMR spectrum of compound DPP3A in CDCl<sub>3</sub>.

## 11. References

- [1] J. Shi, S. Zheng, *Macromolecules*. **2001**, *34*, 6571-6576.
- [2] a) A. D. Becke, *J. Chem. Phys.*, 1993, **98**, 5648-5652; b) M. C. R. Delgado, E. G. Kim, D. A. da Silva Filho, J. L. Brédas, *J. Am. Chem. Soc.* **2010**, *132*, 3375-3387; c) L. Wang, B. Xu, J. Zhang, Y. Dong, S. Wen, H. Zhang, W. Tian, *Phys. Chem. Chem. Phys.* **2013**, *15*, 2449-2458.